Cancer Letters 442 (2019) 396–408

Contents lists available at ScienceDirect

Cancer Letters

journal homepage: www.elsevier.com/locate/canlet

Original Articles

Intratumoral injection of gels containing losartan microspheres and (PLG-g-mPEG)-cisplatin nanoparticles improves drug penetration, retention and anti-tumor activity

Meiling Yu[a], Chunxue Zhang[a], Zhaohui Tang[b], Xing Tang[a,*], Hui Xu[a,**]

[a] Shenyang Pharmaceutical University, Benxi, 117004, PR China
[b] Changchu Institute of Applied Chemistry, Chinese Academy of Sciences, Changchu, 130022, Jilin, PR China

ARTICLE INFO

Keywords:
Cisplatin nanoparticles
Losartan microspheres
Intratumoral injection
Collagen inhibition
Intratumoral penetration and drug retention

ABSTRACT

Intratumoral injection of chemotherapy agents may be employed in the treatment of cancers. However, its anti-tumor efficacy is significantly impeded by collagen fibers in the tumor which decrease drug penetration into the tumor tissues. To improve the penetration, collagen inhibiting drug exposure is required. In this study, microspheres were fabricated by the modified double emulsion-solvent evaporation method as the drug delivery system of losartan potassium (LP MSs), with 5% gelatin as the inner phase. The collagen inhibiting experiment analyzed by Sirius Red stains demonstrated that LP MSs may effectively inhibit collagen I synthesis in B16 tumors. In addition, 15% F127 was used as the solvent to fix the formulations at the injection site, with poly (α-L-glutamate) grafted polyethylene glycol mono methyl ether (PLG-g-mPEG)-cisplatin loaded nanoparticles (CDDP NPs) as the model drug. The *in vivo* live imaging system showed that formulations dissolved in 15% F127 had 54.91% CDDP NPs retained in tumors at the end of 10 days, in comparison with 19.72% for those solved in water, suggesting strong intratumoral retention property of the *in situ* gel. In addition, confocal laser scanning microscope (CLSM) and Energy-Dispersive Analysis of X-ray spectroscopy combined with scanning electron microscope (SEM-EDAX) tests showed that LP MSs can effectively enhance the distribution and penetration of CDDP NPs within tumors. Furthermore, tumors i.t. treated with LP MSs/CDDP NPs gel could be significantly halted, or even reduced to 200 mm^3, comparing with a volume of about 12000 mm^3 incontrol group at the end of the anti-tumor effect experiment. These results provided important guiding principles for prolonged and localized drug delivery system of intratumoral collagen inhibitor. The improvements of intratumoral penetration method made in this study provided practical significance for the treatment of cancer, especially for mass tumors.

1. Introduction

For decades, cancer has been one of the life-threatening diseases [1]. Theoretically, cancers can heal if tumor cells are removed completely. Surgery is one of the most frequently used treatments, especially for early stage solid tumors that have not yet tightly adhered to the surrounding tissues and large vessels. However, when cancer diagnosis is made, often it is no longer at the early stage, and options of surgical treatment are always limited. In such cases, chemotherapy/radiotherapy, immune therapy, and photodynamic therapy are therefore chosen in clinical practices [2–5]. These therapies are intended to deliver the active substance to the cancerous lesion location, and studies have shown satisfying results [6–10]. However, although these therapies are either active or passive tumor targeting, there are severe side effects after systemic administration of anticancer drugs due to their toxicity on normal tissues [11].

Since the primary goal of clinical treatment for tumors is to enhance anti-cancer effect and reduce systemic toxicity, local treatment such as intratumoral therapy has attracted increasing interests. Different from systemic administration, intratumoral drugs stay in the lesion for a long time [12–14], thus achieving the desired anti-tumor activity. Intratumoral therapy is a tumor therapeutic approach that not only directly delivers chemotherapeutic drugs, immune antibodies or other therapeutic substances into tumor tissues, but also prevents the host from systemic adverse effects. Intratumoral agents are usually designed to promote a proinflammatory milieu within the tumor microenvironment, recruit effector cells, and inhibit regulatory and suppressor cells. For example,

* Corresponding author. School of Pharmacy, Shenyang Pharmaceutical University, Benxi, 117004, PR China.
** Corresponding author.
E-mail addresses: tanglab@126.com (X. Tang), xuhui-spu@163.com (H. Xu).

https://doi.org/10.1016/j.canlet.2018.11.011
Received 2 June 2018; Received in revised form 3 October 2018; Accepted 8 November 2018

oncolytic virus was widely used in intratumoral administration to kill tumor cells and block the growth of the blood vessels in tumors [15].

Intratumoral injection of chemotherapeutic agents may increase the concentration of drugs within the tumor and inhibit the distribution of the drugs into non-target organs, and therefore, to enhance tumor toxicity and increase antitumor efficacy [16]. It is a promising therapy because the injection may be administered into many tumors. However, due to the high density and high pressure of the tumor matrix, the drug injected through a needle can be easily squeezed out of the pinprick by the high pressure difference, as the interstitial fluid pressure in solid tumors is uniformly elevated, causing a pinprick leak [17]. Thermo-sensitive polymers that transform from sol to gel state at body temperature may be helpful materials to deliver drugs to tumor tissues. For example, poly(organophosphazene) was used as an injectable system to locate agents to tumors [18]. Temperature responsive Pluronic 407 (F127) hydrogel was also widely investigated for its drug residential property [19].

Despite its potential, intratumoral therapy is still far from satisfactory. An important issue is the poor penetration of agents within tumors. It may be resulted from the dense tumor tissues of high pressure [20,21]. To overcome this problem, intratumoral multipoint injection has been recently investigated in an effort to improve intratumoral drug distribution. In addition, local treatment combined with active substances to improve intratumoral penetration is also a popular approach in cancer therapy. For instance, bromelainis used to degrade the proteins in tumors and thus increase the intratumoral penetration of drugs [22,23]. An anti-fibrotic agent, losartan potassium (LP), may reduce collagens in tumors, which is proved to have an improved effect on intratumoral penetration. However, it takes several days for these substances to take effects on tumors [24]. Additionally, to maintain the antitumor effect, continuous administration of these substances with the combination of chemotherapeutic drugs is required, which makes it difficult to manage intratumoral treatment effectively.

In recent years, novel preparations are increasingly used to improve drug delivery as well as drug loaded property [24]. Controlled release drug delivery system, such as microspheres and nanoparticles may be used to prolong the antitumor effect. In this study, we used poly (α-L-glutamate) grafted polyethylene glycol mono methyl ether (PLG-g-mPEG)-cisplatin loaded nanoparticles (CDDP NPs), combined with prolonged release LP microspheres, as a model of using chemotherapeutic drug in the treatment of cancers. Nanoparticles are used for high penetration property within tumors. In addition, to increase drug retention in the tumor matrix, a hydrogel which has sol-gel transition at elevated temperature (e.g. body temperature) is introduced. As reported previously [19], F127 had satisfactory temperature sensitivity and *in vivo* behaviors, which was used in this study to reside the drugs in tumors. The intratumoral injection of LP microsphere-based hydrogel for localized drug delivery system together with CDDP NPs was evaluated for *in vitro* characteristics and *in vivo* antitumor effects.

2. Materials and methods

2.1. Materials and animals

Losartan potassium (LP) was kindly provided by Beijing Twinluck Pharmaceutical Co., Ltd. (Beijing, China); cis-platin (CDDP) was obtained from Kunming Guiyan Pharmaceutical Co., Ltd. (Kunming, China); poly (α-L-glutamate) grafted polyethylene glycol mono methyl ether (PLG-g-mPEG) was synthesized by Changchun Institute of Applied Chemistry Chinese Academy of Sciences (Changchun, China); PLGA (lactide:glycolide = 75:25, 20kDalton) was purchased from Jinan Daigang Biomaterial Co., Ltd. (Jinan, China); Polyvinyl alcohol (PVA-217SB) was kindly provided by Kuraray Co. Ltd. (Osaka, Japan). Gelatin and Pluronic 407 (F127) were purchased from Sigma-Aldrich (USA). Cy5 NHS ester was purchased from Bioorth Biomaterial Co., Ltd.

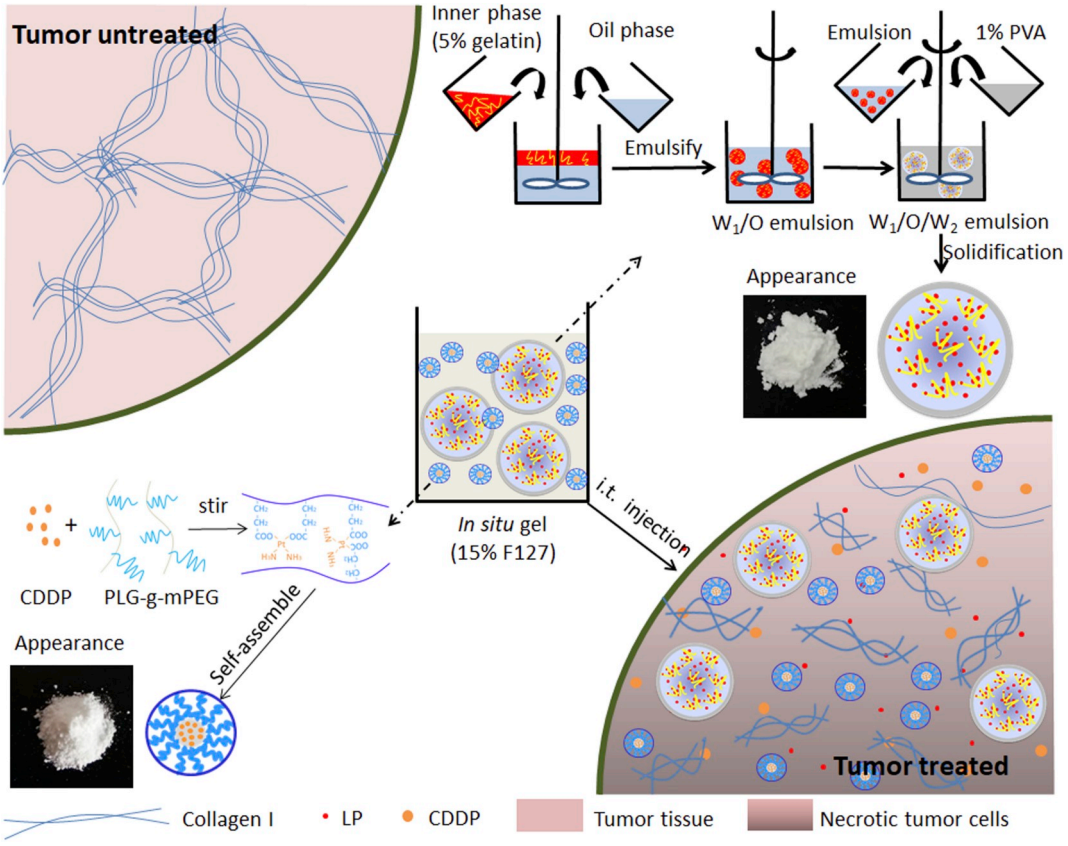

Schematic diagram: Preparation of LP MSs/CDDP NPs co-loaded *in situ* gel, and its collagen inhibition and anti-tumor mechanism by intratumoral injection.

(Nanjing, China). Sirius red was obtained from Beijing Leagene Biomaterial Co., Ltd. (Beijing, China). All other chemicals used were of analytical or chromatographic grade.

B16 mice-derived cancer cells (Melanoma) were purchased from the Cell Bank of Chinese Academy of Science (Shanghai, China); Male C57BL/6 mice (18–20 g, 6 weeks) were obtained from the Experimental Animal Center of Shenyang Pharmaceutical University (Shenyang, China).

All the animal experiments were done in accordance with institution guidelines.

2.2. Preparation of LP MSs

LP loaded PLGA microspheres (LP MSs) were fabricated by a double emulsion-solvent evaporation method with modifications [25]. Briefly, 50 μL of 5% gelatin aqueous solution containing LP (inner aqueous phase, W_1) was added into 1 mL PLGA solution in dichloromethane (oil phase, O). Based on previous investigations, gelatin at the concentration of 5% has the most suitable viscosityfor encapsulating or releasing drugs [26,27]. After homogenizing at 12000 rpm for 1.0 min with a high-speed disperser (ULTRA-TURRAX® T18 digital, IKA Werke GmbH & Co., Staufen, Germany), the formed W_1/O emulsion was then poured into 1% PVA aqueous solution (outer aqueous phase, W_2), which was homogenized for another 2.0 min. The final $W_1/O/W_2$ emulsion was poured into 100 mL deionized water, and the organic solvent was then evaporated at 40 °C under vacuum. The LP MSs were collected by filtration, washed with purified water, and freeze-dried in a FD-1 freeze dryer (LABFREEZ Instruments Co., Ltd., China).

2.3. Microsphere characterization

The microsphere morphology was examined by using BA300 Pol. optical microscope (OM, Motic Ins., Xiamen, China) and S-3400 scanning electron microscope (SEM, Hitachi High Technologies, Kyoto, Japan). Differential scanning calorimetric curves (DSC, Mettler-Toledo AG, Switzerland) and X-ray powder diffraction patterns (XRPD, Shimadzu, Japan) were also measured to characterize the physiochemical properties of the encapsulated drugs. Particle size and size distribution were determined with Laser Particle Size Analyzer (BT-9300S, Better size Co., Ltd., Dandong, China).

To determine the encapsulation efficiency (EE) and drug loading (DL), an aliquot of LP MSs was added to 10 mL volumetric flask. 2 mL DCM was added to break the microspheres, and then deionized water was added to dilute to volume and mixed uniformly. Filtrated through the 0.22 μm filter membrane (Millipore, USA), the solution was then analyzed using the HPLC method (C-18 Column (250 × 4.6 mm, 5 μm) using 0.02% triethylamine in water: acetonitrile (60:40), pH adjusted to 2.5 with O− phosphoric acid as mobile phase at a flow rate of 1.0 mL/min and the detection wavelength was 226 nm) as previously described [28]. The DL and EE were calculated as follows:

$$DL(\%) = \frac{\text{W recovered drug}}{\text{W recovered drug} + \text{W recovered materials}} \times 100\%$$

$$EE(\%) = \frac{\text{W recovered drug}}{\text{W added drug}} \times 100\%$$

2.4. LP release from microspheres

The release of LP from the microspheres was measured using a shaking bath apparatus (ZHWY 110X30, Zhicheng Instrument Co., Shanghai, China) with 5 mL of phosphate buffered saline (PBS, pH 6.8) as the dissolution medium. The microspheres were added in 15% F127 first, and then suspended into PBS or added into PBS directly, incubated at 37 ± 0.5 °C, with the shaking bath vibrating at 100 cycles/min. The release media was removed and refreshed at day 1, 2, 3, 5, 7, 9, 11, 13, 15, 17, 19 and 21 after incubation. The obtained release media was analyzed by HPLC system as described above to determine the amount of released LP.

2.5. Synthesis of poly (α-L-glutamate) grafted polyethylene glycol mono methyl ether (PLG-g-mPEG)-cisplatin nanoparticles (CDDP NPs)

A previously described method was used to prepare the CDDP NPs [29]. First, 20 mg cisplatin (CDDP) was dissolved completely into 6 mL distilled water. 100 mg poly (α-L-glutamate) grafted polyethylene glycol mono methyl ether (PLG-g-mPEG) was dissolved into 4 mL distilled water, and then filtrated through 0.22 μm filter membrane (Millipore, USA). The two solutions were mixed and the mixture was stirred in dark for 48 h to form the nanoparticles. The synthesized preparation was dialyzed (MWCO: 30000 Da) against water for 12 h, and then freeze-dried (LABFREEZ Instruments Co., Ltd., China) to obtain the final CDDP NPs.

The entrapment efficiency was determined by dialysis method. To determine the content of cisplatin in the preparation, the PLG -g-mPEG-CDDP was transformed into free CDDP and then determined by HPLC system (NH_2 Column (250 × 4.6 mm, 5 μm) using acetonitrile: water (75:25) as mobile phase, at a flow rate of 0.8 mL/min and the detection wavelength was 310 nm). CDDPNPs and 0.2 M HCl-0.9% NaCl were transferred into a 10 mL volumetric flask in dark. After shaking at 37 °C for 1 h, the solution was cooled down to room temperature and adjusted to pH 2 ~ 3 with ammonia, 0.9% NaCl was then added to volume. The ultimate solution was analyzed for CDDP.

The particle size and zeta potential of CDDP NPs were measured by dynamic light scattering (DLS, NicompTMPSS380), and the *in vitro* release behavior of CDDP from the nanoparticles was investigated with the method as reported by Jin, L. et al. [30]. The morphology of the nanoparticles was examined by using a transmission electron microscope (TEM, HT-7700, Hitachi, Japan). A drop of the sample with concentration less than 1 mg/mL were put onto a carbon coated copper grid and then negatively stained with 2% phosphotungstic acid for 2 min. The samples were further examined after drying at room temperature.

2.6. Preparation and in vitro characterization of the in situ gels

In this study, F127 was chosen as the gelator of the thermo-responsive gel to enhance the intratumoral drug retention. Rheological behaviors of different concentrations of F127 were performed under a stress-controlled rheometer (DHR-3, TA Instruments, USA) using parallel plates of diameter = 40 mm. The viscosity and temperature curve of the *in situ* gel was measured at the same rotation speed and time span. The samples were loaded at 5 °C and equilibrated at the measurement temperature (starting at 5 °C) and heated up to 40 °C with a step of 5 °C every 10 min. The rotation was fixed at 60r/min for 10s, and then the viscosity was measured at different temperatures.

Certain mass of the prepared microspheres (MSs, equilibrate to 70 mg/mL LP) (20 mg/kg/dwas used according to previous report [41]), nanoparticles (NPs, equilibrate to 10 mg/mL CDDP) (25 mg/kg was chosen as the treatment dose since it was the maximal dose of cisplatin at which mice did not show weight loss throughout the study [32]), or the mixture of micro-nanoparticles (equilibrated to 70 mg/mL LP and 10 mg/mL CDDP) were dispersed in 15% F127 hydrogel to obtain the thermo-responsive *in situ* gels, which was supposed to be able to increase the local drug retention in tumor, as 15% F127 has suitable sol-gel transition temperature that stays in liquid state in lower or room temperature and changes into gel state at higher or body temperature [31].

Structures of F127 containing both LP MSs and CDDP NPs were examined after the suspensions were kept in the refrigerator at 4 °C, shaken to uniform and freeze-dried before imaged by SEM.

2.7. Intratumoral retention of CDDP NPs gels

0.1 mL of B16 cells suspension (7.5×10^6 cells/mL) was injected into the right upper limb of C57BL/6 mice. Approximately 7 days after treatment when the tumor volume reached ~200 mm^3, the mice were randomly divided into two groups. Cy5 labeled CDDP NPs (certain amount of cy5 was added into CDDP NPs solution and the mixture was stirred in dark for 12 h) *in situ* gels and cy5 labeled CDDP NPs solution were respectively administered (i.t., 50 μL, single dose). At predetermined time intervals, i.e., day 0, 1, 2, 4, 6, 8, and 10 after injection, mice were anesthetized with 0.2 mL 4% Chloral hydrate and then photographed using an IVIS Lumina Series III imaging system (Perkin Elmer, USA).

2.8. Intratumoral collagen inhibition

When the tumor volume reached ~400 mm^3, six tumor bearing mice were randomly divided into experimental and control treatment groups. The LP MSs were dispersed into 15% F127 solution (equilibrated to 70 mg/mL LP) and used as the experimental administration, while the 15% F127 solution free of LP was as control treatment. One week after intratumoral administration (50 μL), all the mice were sacrificed and the tumors were collected, fixed in 4% paraformaldehyde, and sectioned for collagen deposition analysis. Samples were stained using Sirius Red to detect collagen I, II and III (Sirius Red is an anionic dye that can strongly bind to collagen molecules). The nuclei of the cells were stained with hematoxylin. The sections were examined using microscope under normal and polarized light, respectively.

2.9. Intratumoral distribution of CDDP NPs

Melanoma bearing mice were randomly divided into 2 groups (n = 3).When the tumor volume reached ~400 mm^3, mice of each group were intratumorally injected with 50 μL of LP MSs and cy5 labeled CDDP NPs gel or cy5 labeled CDDP NPs gel, respectively. A week later, the mice were sacrificed and the tumors were collected, bisected parallel or perpendicular to the needle track, and then frozen sectioned using a FD-1 freeze dryer (LABFREEZ Instruments Co., Ltd., China). After stained with DAPI for cell nucleus, the tumor section was observed by confocal laser scanning microscope (CLSM, ZEISS, LSM 510 SYSTEM, Oberkochen, Germany) to investigate the distribution of CDDP NPs within the tumors.

In the experiment of three groups of tumor bearing mice, when the tumor volume reached ~400 mm^3, mice were treated with LP MSs/CDDP NPs gel (i.t., single dose, equilibrated to 140 mg LP/kg, CDDP 25 mg CDDP/kg); CDDP NPs gel (i.t., single dose, equilibrated to 25 mg CDDP/kg) or CDDP gel (i.t., single dose, equilibrated to 5 mg CDDP/kg). A week later, tumors were collected and bisected parallel the needle track. The bisected halves of the tumors were freeze-dried and then investigated by Energy-Dispersive Analysis with X-ray spectroscopy (SEM-EDAX, Hitachi High Technologies, Kyoto, Japan) to identify the Pt content in different Regions of Interest (ROIs) within the tumors. Since the average length of the tumors was about 10.3 mm with an average volume of about 460 mm^3 at this time, localized measurement was required. Three ROIs at the pinprick of 3 mm, 6 mm and 9 mm were measured respectively. Spectra generated by SEM–EDAX analysis showed peaks corresponding to the elements detected in tumors, and the Pt content was calculated by the ratio of Pt/C at each ROI.

2.10. In vivo antitumor activity and histological study

Tumor-bearing mice were randomly assigned to four treatment groups and one control group ($n = 6$ of each group). When the tumor volume reached ~200 mm^3, the control group received 50 μLof 0.9% NaCl. The other four groups received the following single intratumoral injection respectively: Group 1: LP MSs/CDDP gel (equilibrated to 140 mg LP/kg, and 5 mg CDDP/kg); Group 2: CDDP NPs gel (equilibrated to 25 mg CDDP/kg); Group 3: LP MSs/CDDP NPs solution (equilibrated to 140 mg LP/kg, and 25 mgCDDP/kg); Group 4: LP MSs/CDDP NPs gel (equilibrated to 140 mg LP/kg, and 25 mg CDDP/kg) (These dosages of CDDP were based on what was reported [32]). The body weight and tumor volumes of mice were monitored every 2 days. The tumor volume doubling time (DT) was calculated base on *DT* (day) = $T \times \log 2/(\log V_f - \log V_i)$, where V_f is the final tumor volume, and T is the time interval of the two measurements.

21 days after treatment, mice were sacrificed, and the tumors and their peripheral tissues were collected, sectioned, and stained with hematoxylin and eosin (H&E). Histological images were captured by optical microscope to observe the tumor necrosis region and the inflammatory state of the peripheral muscle tissue.

Table 1
Formulation and physical properties of the microspheres fabricated by traditional and modified methods.

Sample	LP (mg)	PLGA (mg)	DL (%)	EE (%)	Particle size (μm)
Traditional method	300	300	19.67	39.33	18.6 ± 1.3
Modified method	300	300	34.69	69.38	20.4 ± 3.6

2.11. Statistical analysis

Statistical analysis was performed using a paired Student *t*-test to evaluate systemic significant differences.

3. Results

3.1. Physicochemical properties and in vitro release behaviors of LP microspheres

To encapsulate hydrophilic drugs into microspheres, the water-in-oil-in-water (w/o/w) emulsion –solvent evaporation technique has been widely used. Traditional double emulsion technique always yields satisfactory performances, including acceptable entrapment efficiency and feasible release time [33]. However, the efficiency is low to encapsulate the small molecule hydrophilic drug, i.e., LP, into the microspheres prepared by traditional double emulsification-solvent evaporation method (Table 1), which was probably due to the channels left in microspheres that provide routes for drugs to diffuse outside to outer phase [34]. An obvious initial burst release was another main drawback [35]. In this study, gelatin aqueous solution was used as the solvent of the inner water phase which was able to transform the gelatin solution from liquid to gel state by decreasing the temperatures of outer water phase. As such, drugs were fixed in the inner phase, and subsequently the drug entrapment efficiency was increased. In addition, the viscous inner water phase maybe helpful for an effective sustainment of drug release and minimization of initial burst effect [36,37]. Using this modified method, microspheres with higher *DL* and *EE* (34.69% and 69.38%, respectively) was eventually obtained.

The microspheres showed spherical morphology with a typical mean particle size of 20.4 ± 3.6 μm. LP has polymorphisms, with melting points of Tm = 235.47 °C (Form I) and Tm = 273.37 °C (Form II). DSC thermograms and XRPD patterns (data not shown here) showed that LP embedded in microspheres existed as amorphous state. In addition, it was (Fig. 1) indicated that the release of LP from microspheres prepared by the modified double emulsification-solvent evaporation method was extended with less burst release compared to the microspheres prepared by the traditional method. Furthermore, incorporation of the microspheres into temperature-responsive *in situ* gel presented the best release profile among these three preparations.

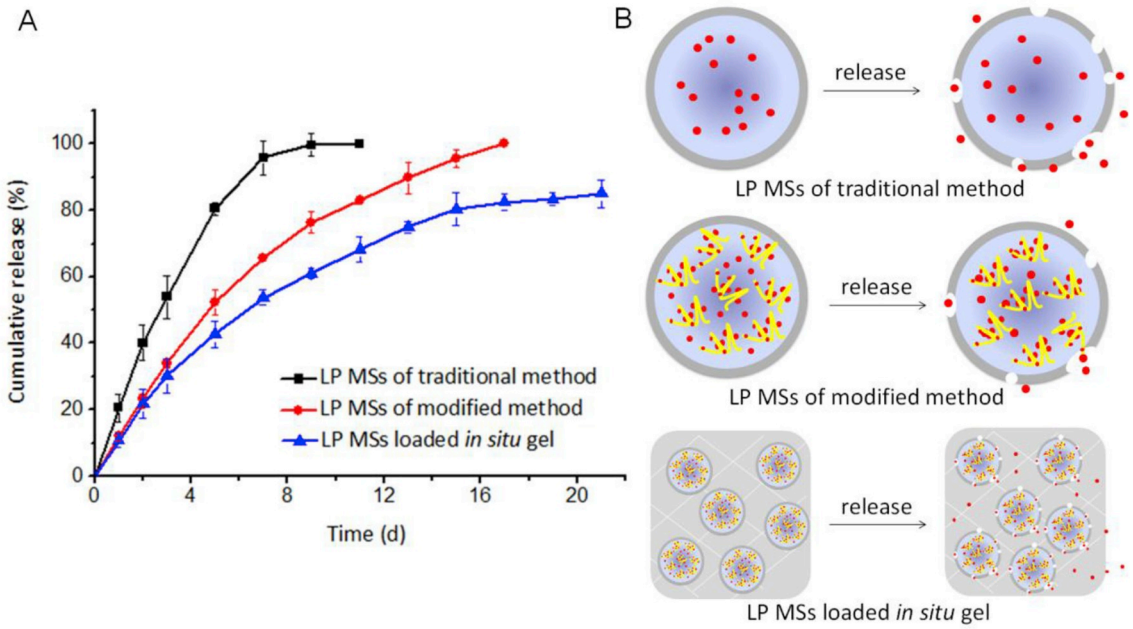

Fig. 1. LP release from microspheres prepared by traditional or modified emulsification – solvent evaporation methods, and from microspheres incorporated in *in situ* gel. (A) Cumulative drug release in the release medium of PBS (pH 6.8) over a period of 21 d (n = 3). (B) Schematics that depict the release behaviors of microspheres fabricated with different methods or microspheres incorporated in gel (LP MSs/CDDP NPs *in situ* gel, equilibrate to 70 mg/mL LP and 10 mg/mL CDDP).

3.2. Physicochemical properties of CDDP NPs and LP MSs/CDDP NPs co-loaded in situ gels

The CDDP NPs were spherical with a mean particle size of about 10 nm and zeta potential of −1.32 mV as shown in Fig. 2 B and Table 2. The EE value (99.25%) suggested that nearly all the CDDP was associated with PLG-g-mPEG. Release behaviors of CDDP NPs solution and the CDDP NPs *in situ* gel were investigated using CDDP solution as a reference. CDDP was released completely from CDDP solution in 8 h with the release amount of 92.86%, while only 4.79%and 2.71% of total CDDP released from CDDP NPs solution and CDDP NPs *in situ* gel at 8 h. The cumulative release rates of CDDP NPs *in situ* gel at day 1 and day 28 were 6.98% and 73.92%, respectively. Compared with CDDP

Table 2
The DL, EE, particle size and Zeta potential of CDDP NPs.

DL (%)	EE (%)	Particle size (nm)	Zeta potential (mV)
16.56	99.25	10.2 ± 2.6	−1.32

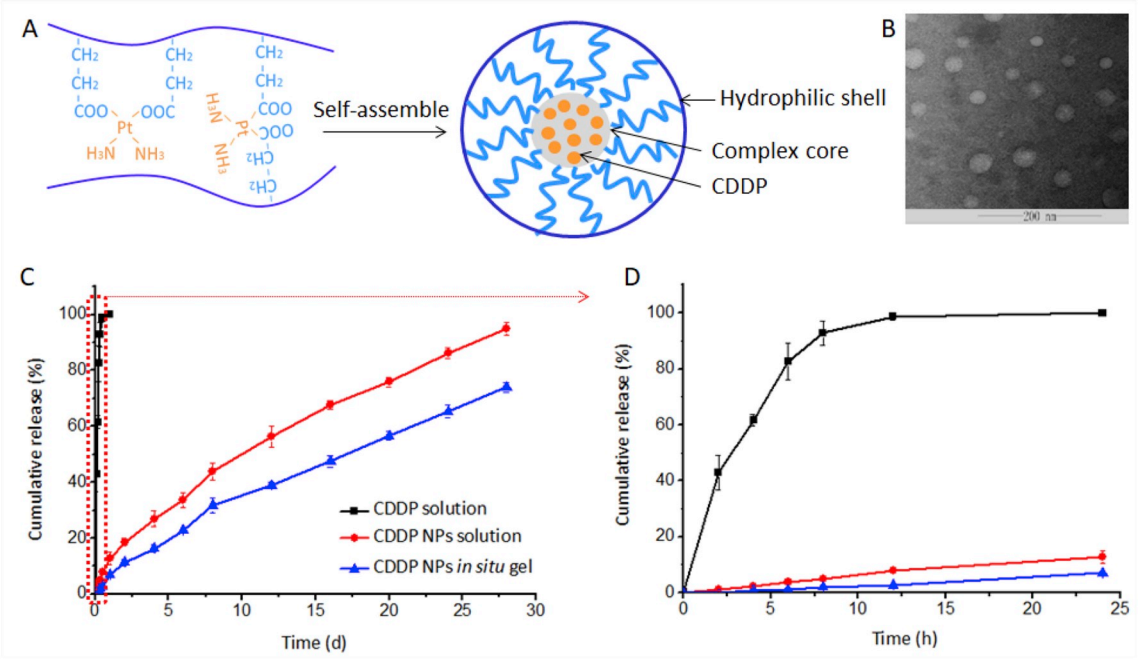

Fig. 2. Self-assembly and release behavior of CDDP NPs. (A) Action of the prepared polymer and its self-assemble mode. (B) Morphology of the nanoparticles observed under TEM. (C) Release profile of CDDP NPsor CDDP NPs incorporated in *in situ* gel (LP MSs/CDDP NPs *in situ* gel, equilibrate to 70 mg/mL LP and 10 mg/mL CDDP) using CDDP solution as reference over a release period of 28 d (n = 3).

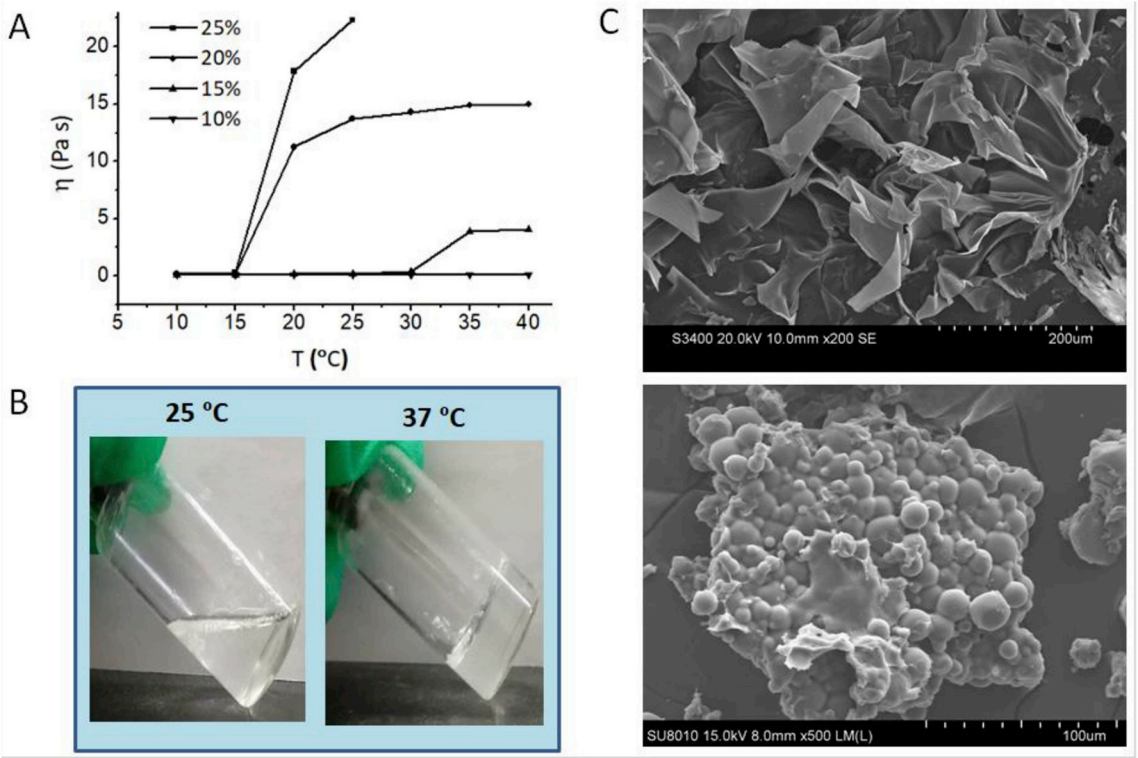

Fig. 3. Characterization of the blank or LP MSs/CDDP NPs co-loaded F127*in situ* gel. (A) Viscosity (η) of different concentrations of F127 (10%, 15%, 20%, 25%) as a function of temperature (T). (B) Photographs of the *in situ* gel at room temperature (25 °C) and at elevated temperature (37 °C), respectively. The gel may display sol-gel conversion at body temperature. (C) SEM graphs of blank 15% F127 (top) and the LP MSs/CDDP NPs co-loaded *in situ* gel (bottom).

solution, the CDDP NPs showed sustained release and no obvious burst effect, making it possible that LP MSs release most LP at the first few days to inhibit intratumor collagen, and CDDP NPs mainly release the CDDP at the following days when it traveled further to kill more tumor cells.

At the same time, the two release curves (LP MSs/CDDP NPs *in situ* gel) showed that in the same gel system, LP was released faster from the microspheres, the cumulative release at day 15 was 80.27%. Therefore, in the early stage of cancer treatment, LP may play a major role in collagen inhibition. By comparison, the release of CDDP NPs was more steady and slow. The cumulative release at day 15 was less than 50%.Because of the different release behaviors, the stable release of CDDP could inhibit the growth of the tumor before and after the LP took effect to inhibit collagen.

The thermo-sensitive property of the LP MSs/CDDP NPs co-loaded *in situ* gel was investigated by rheology analysis, and the $\eta \sim t$ *was shown in* Fig. 3 A. The 15% F127 displayed good fluidity below 30 °C, with viscosity (η) of less than 0.2 Pa*s. The viscosity increased sharply as the temperature rose to about 30 °C, and it became gel state at 37 °C with the η value of about 4.0 Pa*s. The viscosity of 20% or25% of F127 increased abruptly at 15 °C, and tough gels were formed at room temperature, which made the syringe injection difficult. As for 10% F127, it showed no satisfactory temperature sensitivity, and the viscosity was almost unchanged with the increase of temperature.

The SEM images as shown in Fig. 3Calso illustrated the viscosity property of the 15% F127. The blank F127 sample obtained by freeze dry had a densely overlapping structure with folds over the surface, which can firmly embed LP MSs and CDDP NPs, resulting in prolonged release of localized drugs.

3.3. Intratumoral retention of CDDP NPs gels

To prevent the formulation from leaking through the pinprick, 15% F127was used to enhance the viscosity of the preparation and embed the drugs at the site of tumor after injection. In the experimental group with *in situ* gels, the agent was administered immediately after it was taken out from the refrigerator. As shown in Fig. 4 A and B, it remained in liquid state at room temperature, which could be squeezed through the needle smoothly. After injected into tumors, it rapidly converted to a gel state under the higher temperature in the tumor. To test this property, intratumoral retention of two samples was observed in B16 tumor bearing mice using *in vivo* imaging technology with images taken at various time points (Fig. 4 A). Compared with NPs solution, NPs gel showed stronger intratumoral retention property. The majority of cy5 labeled NPs gels stayed in tumors throughout the experiment period, with 54.91% still retained in tumors by end of the observation (Fig. 4B). As to NPs solution, the relative fluorescence intensity reduced greatly at day 1 post injection, with only 19.72% remained at the end of observation.

3.4. Efficacy of collagen inhibition

The LP MSs collagen inhibition efficacy in B16 tumors was evaluated by Sirius Red stain. B16 bearing mice were sacrificed one week after the administration. The tumor tissues were then collected and stained by Sirius Red. Since collagen I is the main component of collagen fiber, and Sirius Red is a strong acid dye which can easily associate with the basic group of collagen molecules and be firmly adsorbed, the stained collagen fibers can very well reflect the content of collagen I [38]. The stained collagen fibers were observed red under OM. Dark red clusters of collagen were observed evenly distributed throughout the region of tumors without LP treatment. In contrast, reduced expression of collagen I were recorded in tumors treated with LP MSs (Fig. 5 A). Polarized light observation showed that collagen fibers had the properties of positive uniaxial birefringence. Combined with Sirius red staining solution, birefringence and resolution may be enhanced so that two types of collagen fibers were differentiated, with

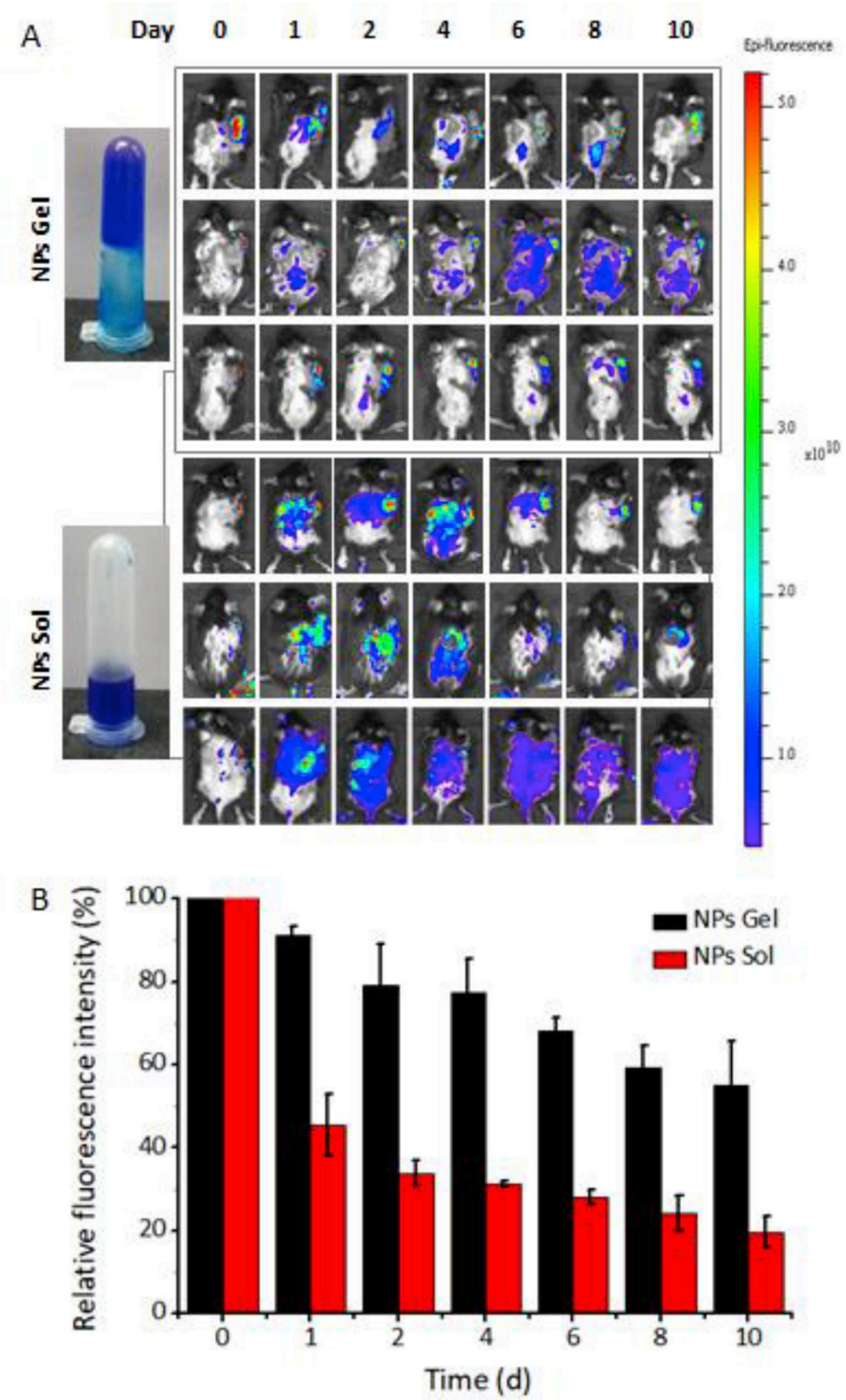

Fig. 4. State and retention of cy5 labeled NPs sol and gel in tumor. (A) Photographs showing the flowing states at body temperature, and fluorescent images showing the retention of cy5 labeled NPs in the tumor after intratumoral injection. (B) Relative fluorescence intensity change in the tumors over a period of 10 days. For group treated with NPs gel, the majority of NPs gel still existed in tumors at the end of the experimental period, while that treated with NPs sol had much less NPs left at day 10.

collagen fiber I showing yellow and collagen fiber III light green. As shown in Fig. 5 B, LP MSs reduced collagen I and III density in tumors. After treated with LP, the content of collagen I and III was decreased when compared with blank group.

3.5. *Effect of LPMSs on the penetration of CDDP NPs in tumor tissues*

All the tumor bearing mice were intratumorally injected with cy5 labeled CDDP NPs gel regardless of the presence of LPMSs. The distribution as well as penetration of the cy5 labeled CDDP NPs was evaluated by CLSM (Fig. 6). A week after the injection, NPs with LP MSs

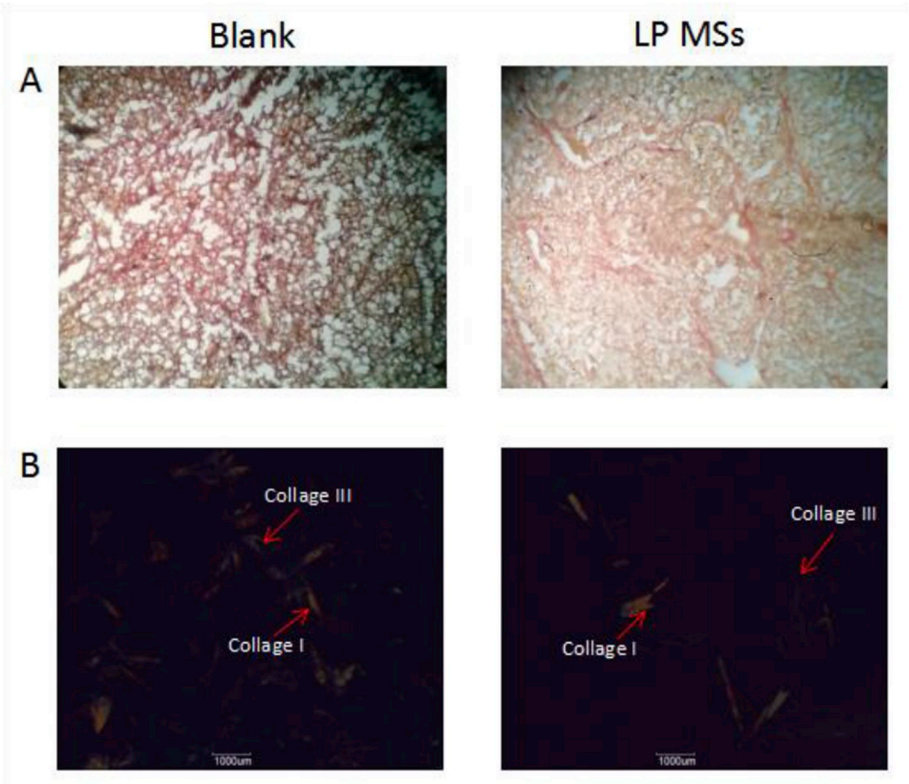

Fig. 5. Collagen fiber content assay in B16 tumors of C57/BL6 mice. (A) Photomicrographs stained with Sirius Red dye. The dark red clusters were observed in blank group, while the color was lighter in experimental group, showing reduced content of total collagen fibers in B16 tumors treated with LP MSs. (B) Images obtained under polarizing microscope showing the content and structures of two different collagen types of collagen I and III. The content of collagen I and III were apparently reduced at day 7 after treated with LP MSs. (For interpretation of the references to color in this figure legend, the reader is referred to the Web version of this article.)

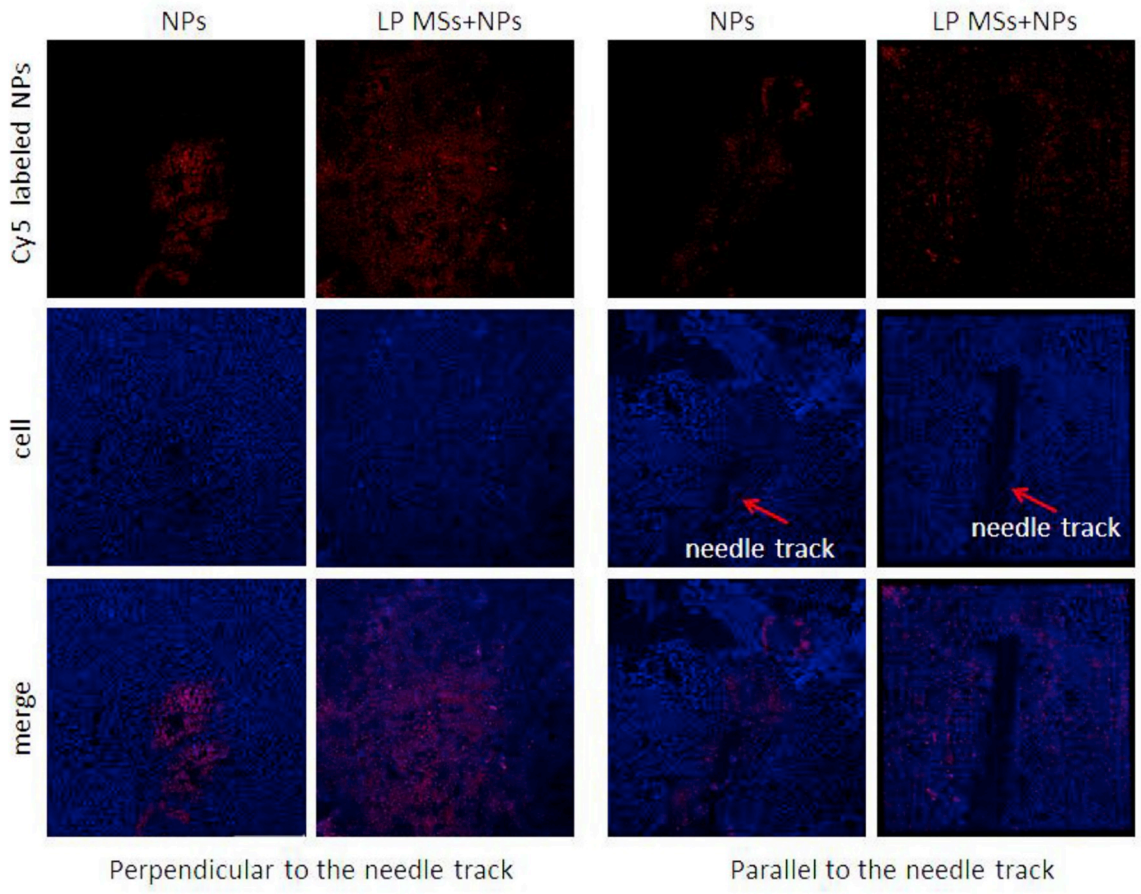

Fig. 6. Fluorescence images showing the distribution of CDDP NPs (red) in tumor tissues. The nuclei of the cells were stained with DAPI (blue). Limited red fluorescence was observed around the needle track in the control group, while widespread distribution of fluorescence was found in tumors that treated together with LP MSs. (For interpretation of the references to color in this figure legend, the reader is referred to the Web version of this article.)

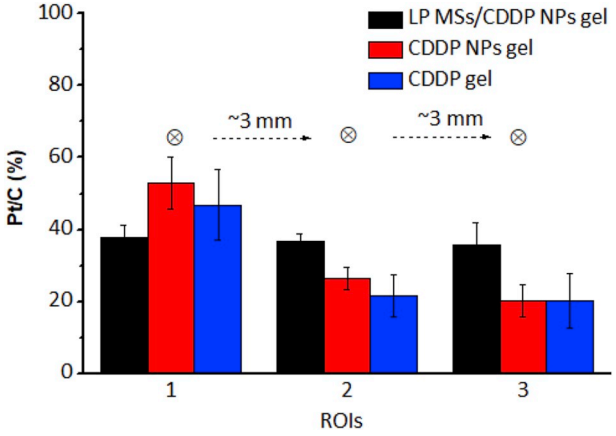

Fig. 7. Investigation of Pt distribution inside the tumor. Pt/C in different regions of interest of tumors was calculated. Not many differences between the content of Pt in different ROIs in the group that treated with LP MSs/CDDP NPs gel, while the regions near the pinprick had more Pt distribution than those far away from the pinprick in group treated only with CDDP NPs gel. But the Pt/C values were similar in the three ROIs between groups of CDDP NPs gel and CDDP gel.

were observed to be distributed widely in tumors. For those NPs without LPMSs, the fluorescence was just observed around the pinprick.

The quantity of Pt in tumor tissues was further investigated by SEM-EDAX technology. Pt accumulation in different regions of interest was determined to evaluate NPs distribution. As shown in Fig. 7, mice treated with LPMSs had better intratumoral drug penetration. The difference of Pt content between the areas close to and far away from the pinprick was less than 3%. However, as for those treated without LP MSs, the difference was 30%, showing a weak intratumoral penetration property.

Although synthesized into NPs, the distribution property of CDDP was not impacted, as both the CDDP NPs gel and CDDP gel had similar Pt content at the same ROI.

3.6. Antitumor efficacy of the agents and histological investigation

The single dose antitumor efficacy of the agents was evaluated in the following manners. B16-bearing mice received one of the five intratumoral injection options: 0.9% NaCl; LP MSs/CDDP gel; CDDP NPs gel; LP MSs/CDDP NPs sol and LP MSs/CDDP NPs gel. Mice were sacrificed at day 21 after the treatment, and tumors were stripped and weighed.

Tumors treated with 0.9% NaCl had a significant transient increase in volume, about 60 times larger than the original volume at the end of investigation (Fig. 8 A, B). In contrast, volume growth was inhibited in tumors treated with LP MSs/CDDP NPs sol (i.t.) and LP MSs/CDDP NPs gel (i.t.). However, compared with LP MSs/CDDP NPs sol, LP MSs/CDDP NPs gel (i.t.) significantly halted or reduced the tumor volume during the treatment, which showed that the *in situ* gel as the carrier of i.t. drug delivery may effectively reduce drug leakage and improve drug retention in tumors. CDDP NPs together with LP MSs was more effective than CDDP NPs alone in inhibiting tumor growth. It was noted that CDDP NPs gel and LP MSs/CDDP NPs gel had similar dose-response patterns of halting tumor growth before day 7, but CDDP NPs gel failed to retard the growth of tumors after day 7. LP MSs/CDDP NPs gel showed continuous prohibition of tumor growth because of the collagen inhibition effect of LP, resulting in lighter tumor weight (Fig. 8 C). In addition, NPs with LP MSs had longer DT as shown in Fig. 8 D. These results suggested that LP MSs remarkably inhibited tumor growth when it was used to treat tumors together with chemotherapeutic drugs. Different from LP MSs/CDDP NPs gel, LP MSs/CDDP gel showed tumor volume increase, which was similar to the blank group after day 3. This is because CDDP was completely released into tumors and was then cleared out, thus failing to halt tumor growth after day 3.In contrast, the CDDP NPs had a sustained release to maintain a stable drug concentration during the treatment.

It was worth noting that body weight in all the experimental or control groups increased over time during the treatment, except the group i.t. supplied with LP MSs/CDDP NPs sol (Fig. 8 E).This was likely due to the fact that formulations dissolved in water were easy to be distributed to the whole body (shown in Fig. 4), thus resulting in side effects and body weight loss.

After the antitumor experiment, all the tumors and surrounding muscles were sectioned and stained with hematoxylin and eosin (H&E), and the morphological changes of the tumors and muscle tissues were shown in Fig. 9. Tumors in blank group had normal cell morphology. It was also shown that the tumors hemorrhaged extensively due to the large size they grew to. Similar image was seen in tumors treated with LP MSs/CDDP NPs gel, except with slight hemorrhage. In mice treated with CDDP NPs gel, only local necrosis was observed in tumors, while in those injected with LP MSs/CDDP NPs sol and LP MSs/CDDP NPs gel, widespread necrotic regions were detected. All these results suggested the CDDP NPs were able to control and prolong the release of CDDP, and LP MSs effectively promoted the intratumoral distribution of CDDP NPs. In addition, the images also showed all groups in the experiments had normal muscle structures except the one treated with LP MSs/CDDP NPs sol. A possible explanation was that the solution had poor retention property and infiltrated into surrounding normal tissues, causing toxicity and resulting in damage to muscle tissues. This was in contrast of the *in situ* gel which had great intratumoral retention property.

4. Discussion

15% F127 used here had a satisfactory temperature-sensitive property. It kept in a very low viscosity (less than 0.5 Pa*S) liquid form at a temperature of below 30 °C. However, when it went above 30 °C, the viscosity increased rapidly to more than 4 Pa*S, making 15% F127 quickly transformed to gel state after being injected into tumors (Fig. 3 A, B). The compact folding structure of 15% F127 gel may firmly embed the micro/nano mixtures together (Fig. 3 C). This helped micro/nanoparticles reside at the sites of tumors and reduced drug leakage from the pinprick (Fig. 10 B). As such, the antitumor effect may be enhanced. Meanwhile, the high viscosity of the *in situ* gel improved drug residence and sustained release as more than half fluorescence-labeled NPs still remained in *in situ* gel in tumors after 10 days of drug administration (Fig. 4).

The prolonged and localized drug delivery system of LP MSs developed in this study may play an important role in inhibiting intratumoral collagen. As previously reported [20,21], tumors, especially fibrotic tumors have plenty of fibers in the tissue where the space left for drug particles are so small that drug penetration is greatly inhibited. The cancer-associated fibroblasts are mainly made up by collagen I which may establish a network that facilitates the invasion of cancer cells [39]. Transforming growth factor is a key factor to reduce drug penetration by inducing collagen I synthesis. Fortunately, LP, an extensively used antifibrotic agent, may meanwhile reduce the synthesis of collagen I with limited safety risks [40,41]. This effect is partly because LP may suppress transforming growth factor-β1 to reduce the levels of collagen I in tumors [40,42]. Themodified LP MSs fabricated in this study showed satisfactory physicochemical characterization. The prolonged release property (Fig. 1) provided possibilities for single administration and made LP long acting in inhibiting collagens content. It was demonstrated that the LP MSs apparently inhibited the collagen I content inmelanoma tumor (Fig. 5). Because of this property, when combined with other chemotherapeutic agents, LP MSs may improve the diffusion of drugs in tumors via inhibiting collagen synthesis. As shown in Figs. 6 and 7, only a wide range of fluorescence or Pt was seen

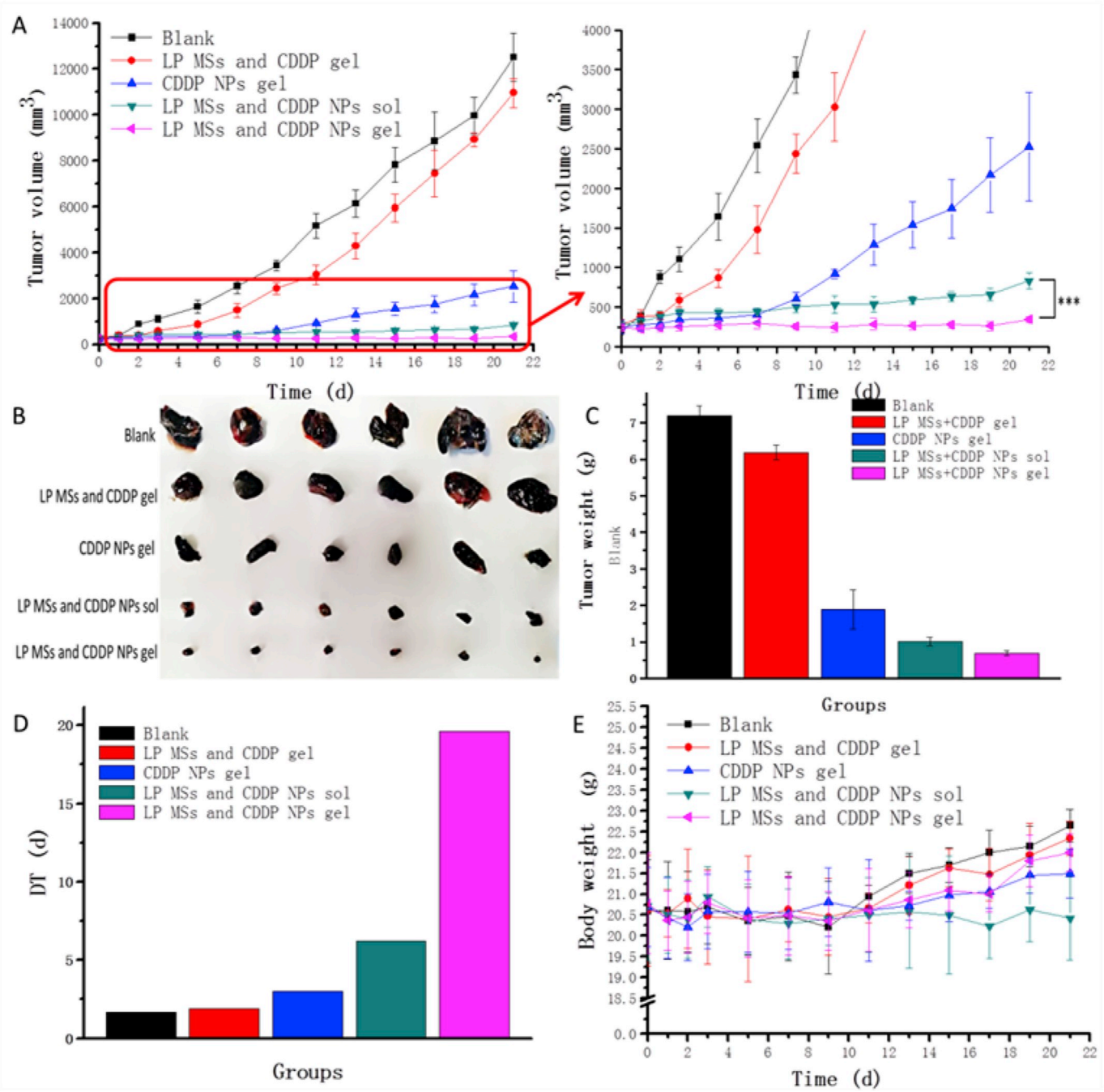

Fig. 8. Antitumor efficacy of intratumoral injection of LP MSs/CDDP NPs *in situ* gel.(A) Relative tumor volume change during the treatment for 21 days. (B) Graph of tumors collected at the end of the experiment. (C) Tumor weights at the end of the experiment. (D) Tumor volume doubling time DT. (E) Relative body weight changes during the treatment. ***$p < 0.001$.

near the needle track without any further distribution in tumors treated without LP MSs. Those tumors injected with LP MSs had fluorescence or Pt throughout the tumor, suggesting that the penetration was strongly improved by LP. Due to the inhibition of collagen synthesis and the destruction of the collagen structure, the once dense collagen network was destroyed, resulting in the enhanced distribution and diffusion of drugs within tumors (Fig. 10). These results clearly demonstrated that LP MSs was an effective and localized agent to inhibit collagen I in tumors, which subsequently facilitated the penetration and distribution of drugs to improving the antitumor effect.

CDDP NPs is another important factor in enhancing intratumoral penetration. Many reports indicated that when administered intravenously, the systemic side effects of CDDP, such as nephrotoxicity and neurotoxicity, were the main reason for its limited use [43,44]. In this study, CDDP NPs was injected intratumorally instead of intravenously. We encapsulated CDDP in PLG-g-mPEG with a ratio of 1:5. The carriers embedded CDDP in the core, which modified physicochemical properties and thus reduced the toxicity of CDDP without impacting its penetrating property as both CDDP NPs gel and CDDP gel had similar Pt content at the same ROI (Fig. 7).

The carboxyl anion (−COO−) on the side chain of PLG -g-mPEG was exchanged with the chloride ion (Cl−) on CDDP and a nucleophilic substitution reaction occurred through the Pt−C coordination bond (Fig. 2 A) to form the CDDP NPs. The complex used the nuclear cross-linking as a hydrophobic core, releasing the drug via exchanging the Chloride ion in tumors, which resulted in the improvement of its

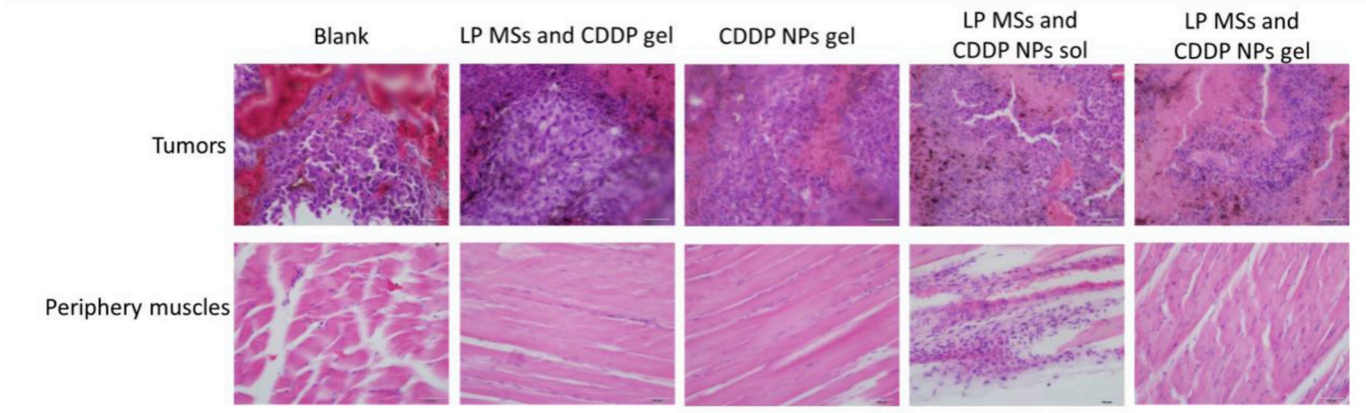

Fig. 9. Histology images of tumors and periphery muscles of mice after intratumoral injection of various formulations. Widespread necrotic cells existed in tumors applied with LP MSs/CDDP NPs sol and LP MSs/CDDP NPs gel, limited locations of necrotic cells were observed in tumors treated with CDDP NPs gel and satisfactory growth state of tumor cells could be seen in blank group and that treated with LP MSs/CDDP gel, with both hemorrhage. All the animals showed normal muscle structures except the one treated with LP MSs/CDDP NPs sol, while with a large number of inflammatory cells.

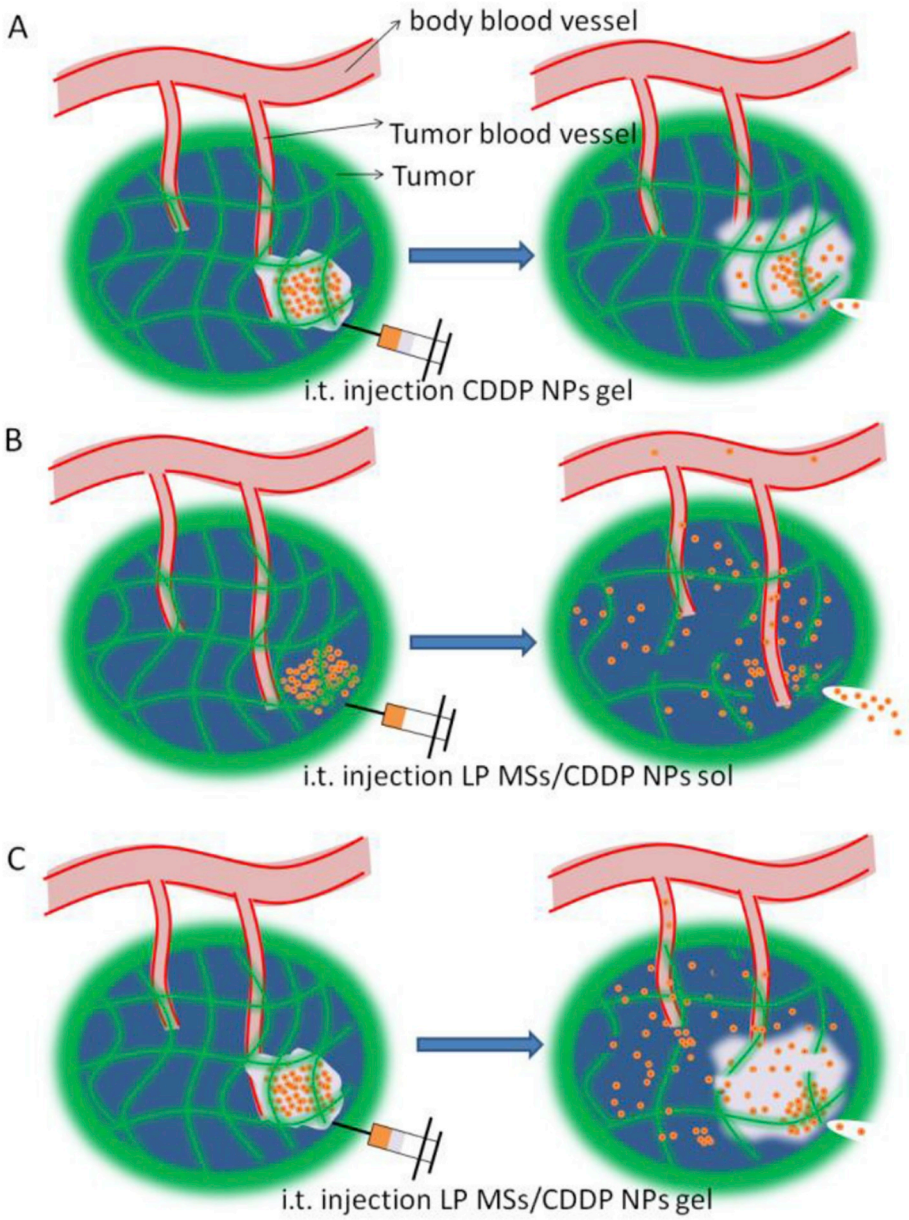

Fig. 10. Schematic diagrams of drug distribution in tumor after intratumoral injection of CDDP NPs gel, LP MSs/CDDP NPs sol, and LP MSs *in situ* gel. The schematic diagrams show how the collagen network structure and *in situ* gel retention affect drug penetration and leakage. The collagen fibers (green) restrict the movement of CDDP nanoparticles (orange) in tumor, and the *in situ* gel (gray) reduce the leakage of drug. (A) When i.t. administrated with CDDP NPs *in situ* gel without LP MSs, large amount of drug stayed near the pinprick, and the dense collagen network structure made it difficult for drugs to penetrate throughout the tumor. (B) When i.t. administrated with LP MSs/CDDP NPs sol, LP treatment destroyed the collagen structure and reduced its content, allowing drug nanoparticles penetrate throughout the tumor tissues, but considerable portions drug leaked out through the pinprick. (C) When i.t. administrated with LP MSs/CDDP NPs *in situ* gel, not only the distribution of drug nanoparticles in tumor was improved, but also the leakage of drug through the pinprick was greatly inhibited. (For interpretation of the references to color in this figure legend, the reader is referred to the Web version of this article.)

physico-chemical stabilization and reliable prolonged delivery by retaining itself in the tumor tissues (Fig. 2 C).The CDDP NPs had negative Zeta potentials of −1.32 mV, which may easily bind to the positive potential at the membrane surface of the tumor cells, providing favorable conditions for nanoparticles to target to tumors. In addition, particle size has been reported to be an important factor of nanoparticle delivery in tumors [45]. Functional and structural studies have shown that large pores exist in tumor vessels that allow nanoparticles to extravasate [46]. Nanoparticles presented a size-dependent inhibition of tumor cell growth. As particle size became smaller, cellular uptake increased in tumor cells and decreased in macrophages [47]. Larger-sized nanoparticles (> 300 nm) were taken up mainly in the spleen and liver via the reticuloendothelial system (RES) [48].Nanoparticles with a size of 10.2 ± 2.6 nm were easily engulfed by tumor cells with increased intratumor penetration and reduced spleen and liver accumulation.

As to the results of *in vivo* antitumor effect, mice treated with LP MSs/CDDP NPs gel had better antitumor effect than LP MSs/CDDP NPs sol. This is likely because the liquid state of LP MSs/CDDP NPs may easily leak from the pinprick and be distributed to blood vessels. Intratumoral retention property was not as good as *in situ* gel, which explained a faster tumor volume increase rate when using LP MSs/CDDP NPs *in situ* gel. Mice i.t. treated with CDDP NPs gel and LP MSs/CDDP NPs gel showed different tumor volume growth patterns. Interestingly, the two groups had comparable profiles before day 7, and they began to differ since then. There are two possible reasons for this: (1) during the first 7 days, tumors were relatively small. Even without the collagen inhibition effect of LP, drugs or NPs could still penetrate widely throughout the tiny tumors. (2) it usually takes several days for LP to take effects [24]. As such, during the first few days after administration, collagen content did not show much difference regardless of LP treatment. But as tumors grew larger, collagen I structure and content in tumors were greatly destroyed and reduced, and CDDP NPs distribution in tumors may therefore be improved. In contrast, tumors without LP treatment still had high collagen density, resulting in limited CDDP NPs penetration, and thus a sharp increase in tumor volume and weight. Regarding LP MSs/CDDP NPs gel and LP MSs/CDDP gel, CDDP NPs had sustained release period for over 21 days in tumors while CDDP was completely released and cleared out within several days resulting in a rapid increase in tumor volume. It is possible, during the initial 21 days, the growth of the tumor impacted on the total body weight. Mice in all groups, except the group treated with LP MSs/CDDP NPs sol, indicated increased body weight at the end of the experiment. After reducing the tumor weight, these mice could keep their body weight or even gain upper body weight when compared with blank group. However, LP MSs/CDDP NPs sol generally caused net body weight loss. This was because liquid state agents were easy to leak from the tumors and went through the whole blood circulation with the NPs staying at the major organs. This may cause body weight loss to a certain degree. As can be observed in Fig. 4, poor intratumoral retention property may make the agents easily diffuse to blood vessels, and then to whole blood circulation as well.

The sections of tumors and surrounding muscles showed that LP MSs/CDDP NPs gelhad the best inhibition effect on tumor cells with no damages to surrounding muscle tissues. The results indicated that LP MSs/CDDP NPs gel presented an improvement in anti-tumor treatment.

5. Conclusion

In this study, a novel strategy was introduced to improve the intratumoral distribution and retention of CDDP NPs in a mouse model of B16 melanoma tumors. To enhance the penetration of CDDP, LP loaded PLGA microspheres were fabricated using a modified emulsion-solvent evaporation method, which inhibited collagen I synthesis through a prolonged time period. Investigations on inhibition of collagen by LP and intratumoral distribution of CDDP confirmed that LP MSs improved the intratumoral accumulation of CDDP in B16 tumors and significantly enhanced the penetration and distribution of CDDP. Additionally, 15% F127 was chosen to localize drug delivery. This *in vivo* study and antitumor efficacy experiment demonstrated that 15% F127 localized LP MSs/CDDP NPs in tumor tissues. CDDP loaded in nanoparticles can prolong drug release while having fewer systemic side effects. This study suggested a novel approach of using intratumoral injection in cancer treatment.

Conflict of interest

There is no conflict of interest of this paper.

All the animal experiments were done in accordance with institution guidelines.

Acknowledgments

This work was partly supported by the Natural Science Foundation of Liaoning Province (201602717).

References

[1] M.R. Stratton, Exploring the genomes of cancer cells: progress and promise, Science 331 (2011) 1553–1558.
[2] N. Schweitzer, A. Vogel, Systemic therapy of cholangiocarcinoma: from chemotherapy to targeted therapies, Best Pract. Res. Clin. Gastroenterol. 29 (2015) 345–353.
[3] S. Gao, et al., Oxygen-generating hybrid nanoparticles to enhance fluorescent/photoacoustic/ultrasound imaging guided tumor photodynamic therapy, Biomaterials 112 (2017) 324.
[4] J. Riba, S.E. de Romani, J. Masia, Neoadjuvant chemotherapy for breast cancer treatment and the evidence-based interaction with immediate autologous and implant-based breast reconstruction, Clin. Plast. Surg. 45 (2018) 25.
[5] M. Toussaint, et al., Proton MR spectroscopy and diffusion MR imaging monitoring to predict tumor response to interstitial photodynamic therapy for glioblastoma, Theranostics 7 (2017) 436.
[6] F. L, et al., Intravenous injection of MVA virus targets CD8+ lymphocytes to tumors to control tumor growth upon combinatorial treatment with a TLR9 agonist, Canc. Immunol. Res. 2 (2014) 1163.
[7] T. Shi, M. Wang, H. Li, et al., Simultaneous monitoring of cell-surface receptor and tumor-targeted photodynamic therapy via TdT-initiated poly-G-quadruplexes, Sci. Rep. 8 (1) (2018) 5551.
[8] P. Sampath, et al., Crosstalk between immune cell and oncolytic vaccinia therapy enhances tumor trafficking and antitumor effects, Mol. Ther. J. Am. Soc. Gene Ther. 21 (2013) 620–628.
[9] H. Yang, et al., Chemo-photodynamic combined gene therapy and dual-modal cancer imaging achieved by pH-responsive alginate/chitosan multilayer-modified magnetic mesoporous silica nanocomposites, Biomater. Sci. 5 (2017).
[10] C. Zhang, J. Ding, B. Wang, P. Chen, A Single Intravenous Injection of Oxycodone Hydrochloride in the Treatment of Acute Post-Operative Pain after Laparoscopic Rectal Tumor Resection vol. 8, (2017), p. 01055.
[11] R.V. Chari, Targeted cancer therapy: conferring specificity to cytotoxic drugs, Accounts Chem. Res. 41 (98) (2008).
[12] A.M. Al-Abd, K.Y. Hong, S.C. Song, H.J. Kuh, Pharmacokinetics of doxorubicin after intratumoral injection using a thermosensitive hydrogel in tumor-bearing mice, J. Contr. Release 142 (2010) 101–107.
[13] H.W. Seo, et al., Injectable intratumoral hydrogel as 5-fluorouracil drug depot, Biomaterials 34 (2013) 2748–2757.
[14] L. Zhao, et al., pH triggered injectable amphiphilic hydrogel containing doxorubicin and paclitaxel, Int. J. Pharm. 410 (83) (2011).
[15] K.A. Streby, et al., Intratumoral injection of HSV1716, an oncolytic herpes virus, is safe and shows evidence of immune response and viral replication in young cancer patients, Clin. Canc. Res. Official J. Am. Assoc. Canc. Res. 23 (2017) 3566.
[16] M. Westphal, et al., A phase 3 trial of local chemotherapy with biodegradable carmustine (BCNU) wafers (Gliadel wafers) in patients with primary malignant glioma, Neuro Oncol. 5 (2003) 79.
[17] M. Akhlaghi, A. Pourjavadi, A.R. Jalilian, Preparation and primary evaluation of 66Ga-DTPA-chitosan in fibrosarcoma bearing mice via intra-tumor injection technique, Iran. J. Nucl. Med. 56 (1) (2011) 41–47.
[18] A.M. Al-Abd, K.Y. Hong, S.C. Song, H.J. Kuh, Pharmacokinetics of doxorubicin after intratumoral injection using a thermosensitive hydrogel in tumor-bearing mice, J. Contr. Release 142 (2010) 101.
[19] M.S.H. Akash, K. Rehman, Recent progress in biomedical applications of Pluronic (PF127): Pharmaceutical perspectives, J. Contr. Release (2015) 209120–209138.
[20] S. Kakkad, Collagen 1 Fibers and Hypoxic Tumor Microenvironments in Breast Cancer and Their Effect on Transport of Molecules within the Tumor Matrix, (2013).
[21] A. Uchugonova, et al., Multiphoton tomography visualizes collagen fibers in the tumor microenvironment that maintain cancer-cell anchorage and shape, J. Cell. Biochem. 114 (99) (2013).

[22] K. Pillai, J. Akhter, T.C. Chua, et al., Anticancer property of bromelain with therapeutic potential in malignant peritoneal mesothelioma, Canc. Invest. 31 (4) (2013) 241–250.
[23] R. Nasiri, et al., Targeted delivery of bromelain using dual mode nanoparticles: synthesis, physicochemical characterization, in vitro and in vivo evaluation, RSC Adv. 7 (2017) 40074–40094.
[24] O. Qutachi, E.J. Wright, G. Bray, O.A. Hamid, F.R.A.J. Rose, K.M. Shakesheff, D. Delcassian, Improved delivery of PLGA microparticles and microparticle-cell scaffolds in clinical needle gauges using modified viscosity formulations, Int. J. Pharm. 546 (1–2) (2018) 272–278.
[25] M. Yu, et al., Core/shell PLGA microspheres with controllable in vivo release profile via rational core phase design, Artif. Cell. Nanomed. Biotechnol. 1–10 (2018).
[26] V. Vijayakumar, K. Subramanian, Diisocyanate mediated polyether modified gelatin drug Carrier for controlled release, Saudi Pharmaceut. J. 22 (1) (2014) 43–51.
[27] N. Tinne, B. Kaune, A. Krüger, T. Ripken, Single Snapshots of the Cavitation Bubble Interaction Dynamics in a 5% Porcine Gelatin Solution, (2014).
[28] P.R. Patil, S.U. Rakesh, P.N. Dhabale, K.B. Burade, RP- HPLC method for simultaneous estimation of losartan potassium and amlodipine besylate in tablet formulation, Int. J. Chemtech Res. 1 (2009) 464–469.
[29] H. Yu, et al., Pharmacokinetics, biodistribution and in vivo efficacy of cisplatin loaded poly(L-glutamic acid)-g-methoxy poly(ethylene glycol) complex nanoparticles for tumor therapy, J. Contr. Release 205 (2015) 89–97.
[30] I.D.M. Azmi, J. Østergaard, S. Stürup, B. Gammelgaard, A. Urtti, S.M. Moghimi, A. Yaghmur, Cisplatin encapsulation generates morphologically different multicompartments in the internal nanostructures of nonlamellar liquid-crystalline self-assemblies, Langmuir 34 (22) (2018) 6570–6581.
[31] P.G. Yeole, D. Iyer, Thermosensitive in situ gel of Timolol Maleate for the treatment of open angle glaucoma, Res. J. Pharmaceut. Biol. Chem. Sci. 2 (2011) 1048–1064.
[32] A. Shikanov, S. Shikanov, B. Vaisman, J. Golenser, A.J. Domb, Cisplatin tumor biodistribution and efficacy after intratumoral injection of a biodegradable extended release implant, Int. J. Pharm. 358 (2011) 114–120.
[33] S. Tamnak, et al., Encapsulation properties, release behavior and physicochemical characteristics of water-in-oil-in-water (W/O/W) emulsion stabilized with pectin–pea protein isolate conjugate and Tween 80, Food Hydrocolloids 61 (2016) 599–608.
[34] M. Li, O. Rouaud, D. Poncelet, Microencapsulation by solvent evaporation: state of the art for process engineering approaches, Int. J. Pharm. 363 (2008) 26–39.
[35] J.H. Park, M. Ye, K. Park, Biodegradable polymers for microencapsulation of drugs, Molecules 10 (2005) 146–161.
[36] D.Y. Kim, et al., Synergistic anti-tumor activity through combinational intratumoral injection of an in-situ injectable drug depot, Biomaterials 85 (2016) 232–245.
[37] L. Deng, X. Kang, Y. Liu, F. Feng, Z. Hui, Effects of surfactants on the formation of gelatin nanofibres for controlled release of curcumin, Food Chem. 231 (2017) 70–77.
[38] S. Gupta, et al., Picrosirius red: a better polarizing stain, J. Histotechnol. (2017) 1–8.
[39] R.C. G, G. Bernard, S. Tremblay, et al., Exosomes induce fibroblast differentiation into cancer-associated fibroblasts through TGFβ signaling, Mol. Canc. Res. 078 (2018) molcanres.0784.2017.
[40] Q.Q. Fang, X.F. Wang, W.Y. Zhao, et al., Angiotensin-converting enzyme inhibitor reduces scar formation by inhibiting both canonical and noncanonical TGF-β1 pathways, Sci. Rep. 8 (1) (2018).
[41] B. Diop-Frimpong, V.P. Chauhan, S. Krane, Y. Boucher, R.K. Jain, Losartan inhibits collagen I synthesis and improves the distribution and efficacy of nanotherapeutics in tumors, Proc. Natl. Acad. Sci. U.S.A. 108 (2011) 2909–2914.
[42] C. Hu, X. Liu, R. Wei, et al., Regulating cancer associated fibroblasts with losartan-loaded injectable peptide hydrogel to potentiate chemotherapy in inhibiting growth and lung metastasis of triple negative breast cancer, Biomaterials 144 (2017) 60–72.
[43] F. Guo, L. Xu, S. Gao, et al., Effect of orexin-A in the arcuate nucleus on cisplatin-induced gastric side effects in rats, Neurosci. Res. (2018), https://doi.org/10.1016/j.neures.2018.06.001.
[44] F. Guo, L. Xu, S. Gao, et al., Effect of orexin-A in the arcuate nucleus on cisplatin-induced gastric side effects in rats, Neurosci. Res. (2018), https://doi.org/10.1016/j.neures.2018.06.001.
[45] A. Albanese, P.S. Tang, W.C. Chan, The effect of nanoparticle size, shape, and surface chemistry on biological systems, Annu. Rev. Biomed. Eng. 14 (1) (2011) 1.
[46] T. Stylianopoulos, Intelligent drug delivery systems for the treatment of solid tumors, Eur. J. Nanomed. 8 (1) (2016) 9–16.
[47] J.S. Choi, et al., Size-controlled biodegradable nanoparticles: preparation and size-dependent cellular uptake and tumor cell growth inhibition, Colloids Surfaces B Biointerfaces 122 (2014) 545–551.
[48] H. Kim, S. Lee, H. Jeong, D. Kim, Enhanced tumor targetability of PEGylated mesoporous silica nanoparticles on in vivo optical imaging according to their size, RSC Adv. 4 (2014) 31318–31322.